



---

*Research article*

## The influence of pulse current duty cycle on the tensile deformation behavior of commercially pure titanium

Vladimir Stolyarov\* and Oleg Korolkov

Mechanical Engineering Research Institute of Russian Academy of Sciences, Moscow, Russia

\* **Correspondence:** Email: [vlstol@mail.ru](mailto:vlstol@mail.ru); Tel: +7-495-625-60-28.

**Abstract:** This article examined the influence of pulse current duty cycle at different pulse durations and frequencies on the ratio of thermal and true electroplastic effects (EPEs) during quasi-static tension testing of commercially pure Grade 2 titanium in a coarse-grained recrystallized state. Duty cycle values varied over a wide range corresponding to the minimum thermal effect of the current. Microstructural studies were performed using optical microscopy, microhardness analysis of various sections of the specimen, and scanning electron microscopy of the fracture surface. An increase in temperature, a decrease/increase in the amplitude of stress surges, a reduction in flow stress, ductility, and suppression of the twinning mechanism with a decrease in the duty cycle in the range of 1000–50,000 were demonstrated. In all cases, the failure mechanism remained ductile but changed from dimple type to predominantly cup type with a simultaneous increase in porosity. The use of the duty cycle parameter allows one to regulate the contribution of thermal and electroplastic effects, which can be useful both for modeling the EPE mechanism and for practical use in pressure processing of titanium alloys accompanied by current.

**Keywords:** titanium; tension; pulse current; duty cycle; microstructure; microhardness; fracture

---

### 1. Introduction

In conductive materials, electric current has a significant impact on their structure and mechanical behavior, contributing to the manifestation of the electroplastic effect (EPE) [1,2]. The mode (direct, alternating, and pulsed) and regimes (density, frequency, pulse duration) of the current are of great importance. Relatively recently, studies and even reviews have begun to appear that examined the role

of not only the main current modes but also the duty cycle of the pulsed current during the tension of various materials: iron [3], niobium [4], aluminum bronze [5], and copper and magnesium alloys [6]. These studies have shown that increasing the duty cycle can increase the contribution of the EPE and, accordingly, reduce the thermal effect of the current. It is noted that most foreign studies use low duty cycle values, possibly due to the practical need to increase ductility. A number of studies have examined the influence of pulsed current modes and tensile conditions on EPE. The authors of [7] examined the mechanical behavior of an aluminum alloy under tension with a high-duty cycle pulsed current and corresponding structural changes. It was found that under the influence of electric current, elongation increased sharply as the flow stress decreased. Microstructural observations confirmed that the influence of Joule heating on mechanical behavior was not dominant, but dislocation annihilation did occur. In [8], it was shown that even the rigidity of the testing machine significantly affects the reduction of flow stress, the absolute value of which in the elastic region is primarily due to thermal effects. For cold-formed and homogenized duplex stainless steel, it was shown that reducing the duty cycle and increasing the current density and pulse duration reduces flow stress by 25%–30% compared to tension without current while maintaining sufficient ductility [9].

The study of EPE in titanium and its alloys is of particular interest, primarily due to their use as biomaterials for medical implants. It is believed that the use of pulsed current during the molding of titanium components will improve deformability, reduce deformation temperatures, and eliminate adhesion and oxidation on the surface of the semi-finished product [3,4]. The role of the current duty cycle in this regard is difficult to overestimate, as it is the parameter that regulates the ratio of the two main contributions of the pulsed current: thermal and purely electroplastic [10]. An analysis of the duty cycle shows that identical values of this parameter can be achieved by varying either the frequency (at a constant pulse duration) or the pulse duration (at a constant frequency). However, it is unclear whether the structural changes, deformation behavior, and mechanical properties of the material will be identical for the same duty cycle but achieved using different combinations of pulse duration and frequency. The aim of this work is to establish patterns in changes in microstructure, deformation behavior, mechanical properties, and fracture mechanisms during tension of coarse-grained titanium, accompanied by a pulsed current of varying duty cycle.

## 2. Materials and methods

The research material was commercially pure Grade 2 titanium in a coarse-grained condition in the form of a 2 mm diameter wire in an annealed (850 °C/2 h, HV100 = 145) condition with an average recrystallized grain size of  $d = 200 \mu\text{m}$  (Figure 1). The chemical composition according to the certificate is given in Table 1.

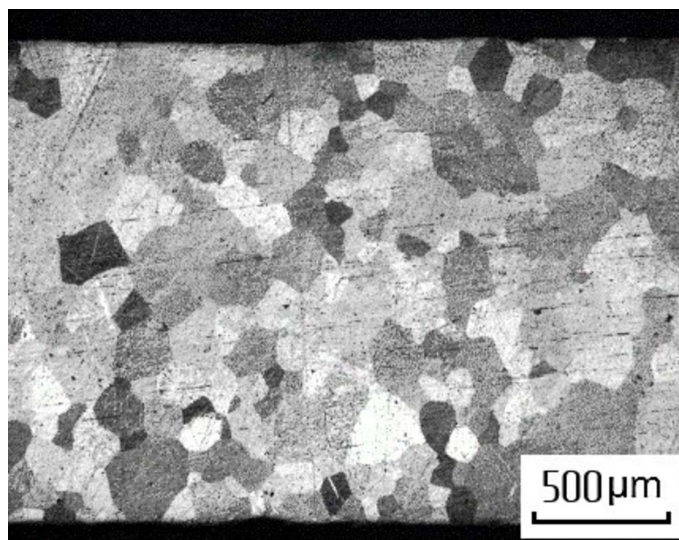


**Figure 1.** Microstructure of Grade 2 titanium in the original state.

**Table 1.** Chemical composition of Grade 2 titanium (wt.%).

Material	N	C	H	Fe	O	Ti
Grade 2	0.02	0.04	0.012	0.25	0.22	rest

Tensile tests were performed on an IR-5081/20 horizontal tensile testing machine. Elongation was estimated at a gage length of  $l_0 = 25$  mm. The tensile rate was 0.8 mm/min ( $1.3 \times 10^{-3} \text{ s}^{-1}$ ). Tensile tests were conducted without current and with pulsed current in various modes. For each mode, at least three samples were used. The amplitude current density ( $j$ ) in all experiments was chosen to be  $j = 1000 \text{ A/mm}^2$ , which ensured the observation of downward stress drops for all pulse durations ( $\tau$ ) used in the range  $\tau = 100\text{--}1000 \text{ }\mu\text{s}$  and current frequencies in the range 0.07–1 Hz. This allowed studying the effect of duty cycle ( $Q$ ) =  $t/\tau = 1/\nu$  (where  $t$  and  $\nu$  are the pulse period and frequency) over a wide range from 1000 to 50,000. The duty cycle values considered correspond predominantly to the region where the sample temperature ( $T$ ) does not exceed 180 °C and is not capable of leading to noticeable structural changes. Specific current modes are listed in Tables 2 and 3.

**Table 2.** Current modes at constant pulse duration.

No.	Condition	$\nu$ (Hz)	$j$ (A/mm <sup>2</sup> )	$\tau$ ( $\mu\text{s}$ )	$Q$
1	No current	-	1000	1000	-
2	Pulse current	0.07			15,000
3		0.1			10,000
4		0.2			5000
5		0.5			2000
6		1			1000

**Table 3.** Current modes at constant frequency.

No.	Condition	$\tau$ ( $\mu\text{s}$ )	$j$ ( $\text{A}/\text{mm}^2$ )	$\nu$ (Hz)	Q
1	No current	-	1000	0.2	-
2	Pulse current	100			50,000
3		200			25,000
4		500			10,000
5		800			6250
6		1000			5000

Electric current from the pulse generator was fed through the busbars to the wire grips of the testing machine. To monitor the current parameters, a shunt was located on the negative busbar, connected to a digital oscilloscope INSTRUSTAR ISDS205. The specimen grips were insulated from the machine using fiberglass spacers. Specimen temperature during tension was measured using a UNI-T Digital Thermometer UT320 Series with a connected chromel–alumel thermocouple located in the specimen center with an accuracy of  $\pm 0.5\%$ . The sampling rate of a digital thermometer's thermocouple is 4 measurements per second.

The setup diagram and pulse shape are shown in Figure 2.

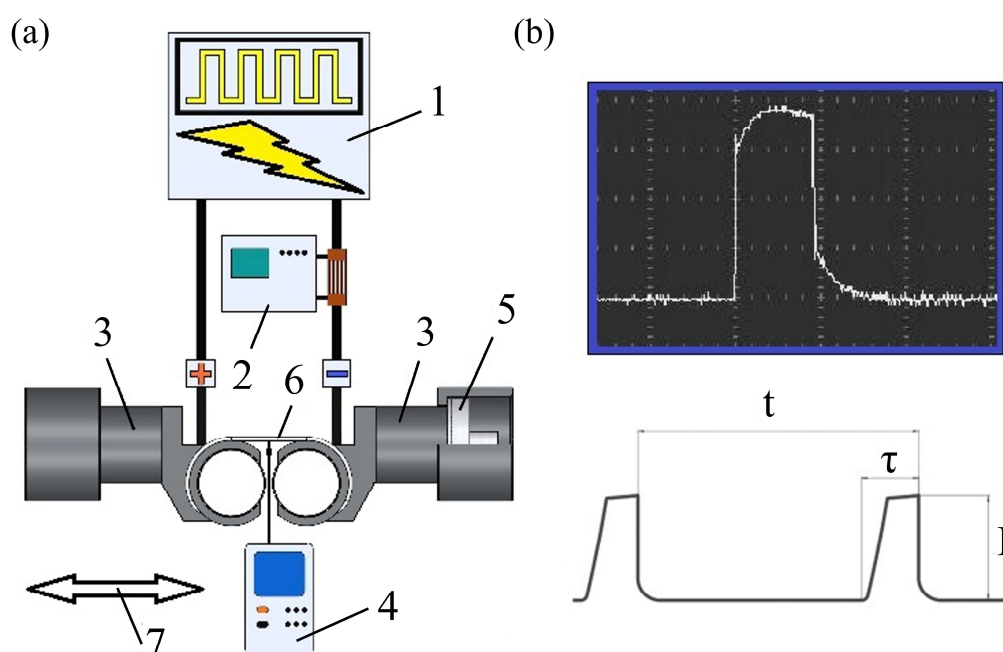


**Figure 2.** (a) Schematic diagram of the test setup and (b) an example of an oscillogram illustrating the shape of a current pulse with a duration of  $\tau = 100\text{--}1000 \mu\text{s}$ , 1: pulse current generator; 2: oscilloscope; 3: clamps; 4: millivoltmeter (digital thermometer); 5: insulation; 6: sample; 7: tension direction.

The electroplastic effect was assessed by the relative decrease in ultimate tensile strength  $\Delta\sigma_{\text{UTS}}$  and by the relative change in the amplitude of the stress jump  $\Delta\sigma_a$ . The difference in flow stresses was calculated using the Eq 1:

$$\Delta\sigma_{\text{UTS}} = \frac{(\sigma_{\text{UTS}} - \sigma_{\text{UTS}}^{\text{EPE}}) \times 100\%}{\sigma_{\text{UTS}}} \quad (1)$$

where  $\sigma_{\text{UTS}}$  and  $\sigma_{\text{UTS}}^{\text{EPE}}$  are the ultimate tensile strength without and with current.

The relative change in the amplitude of the stress jump under the influence of a single current pulse was calculated using Eq 2:

$$\Delta\sigma_a = \frac{\sigma_a}{\sigma_T} \times 100\% \quad (2)$$

where  $\sigma_a$  is the amplitude of the current stress jump, and  $\sigma_T$  is the current stress at the moment the pulse is applied.

The effect of the magnetic field was not considered, since the magnetic induction and induced stress change for the maximum current mode did not exceed 0.1 T and 0.5 MPa, respectively.

The microstructure of the specimens was examined before and after tension near the fracture zone in the cross-section using optical microscopy on a Dr. Focal microscope at  $\times 500$  magnification. Specimens were cut using the electron beam cutting method and then mechanically prepared by grinding, polishing, and chemical etching in a mixture of hydrofluoric and nitric acids in water at a ratio of 1:3:6.

Microhardness was measured using a MicroVicky VH1010 instrument; the indenter load was 0.98 N, and the hold time was 10 s. Microhardness measurements after tension were taken in longitudinal cross-sections in areas corresponding to the neck and uniform elongation. At least 10 measurements were taken at each point, with a total error of 5%.

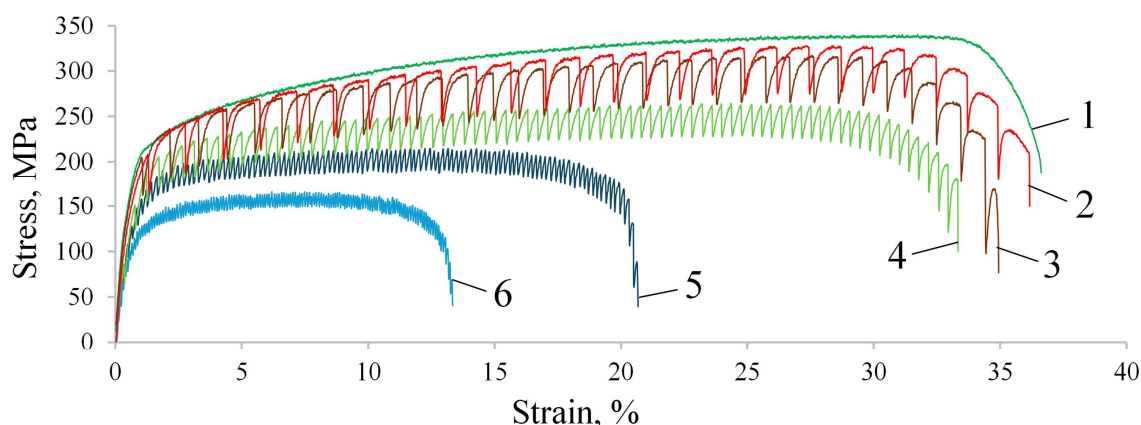
Fractographic images of the fracture surface were obtained using a Tescan Mira 3 LMU scanning electron microscope. In some cases, for improved contrast, specimens were mounted at an angle of  $60^\circ$  to the loading axis.

### 3. Results

When studying the influence of pulsed current duty cycle, not only is the ratio of the kinetic parameters frequency and pulse duration important, but also the absolute values of each. In this study, the duty cycle varied either by changing the frequency (at a constant pulse duration) or by changing the pulse duration (at a constant frequency). Therefore, the results of the influence of both parameters of the duty cycle are presented below.

#### 3.1. At a constant pulse duration

Figure 3 shows stress–strain curves with different values of current duty cycle (at the same current density and pulse duration). Decreasing the duty cycle from  $Q = 15000$  to  $Q = 1000$  reduces the flow stress, relative elongation before failure, and jump amplitude (curves 2, 3, 4, 5, 6). Another effect of decreasing the duty cycle is a decrease in the strain hardening coefficient.



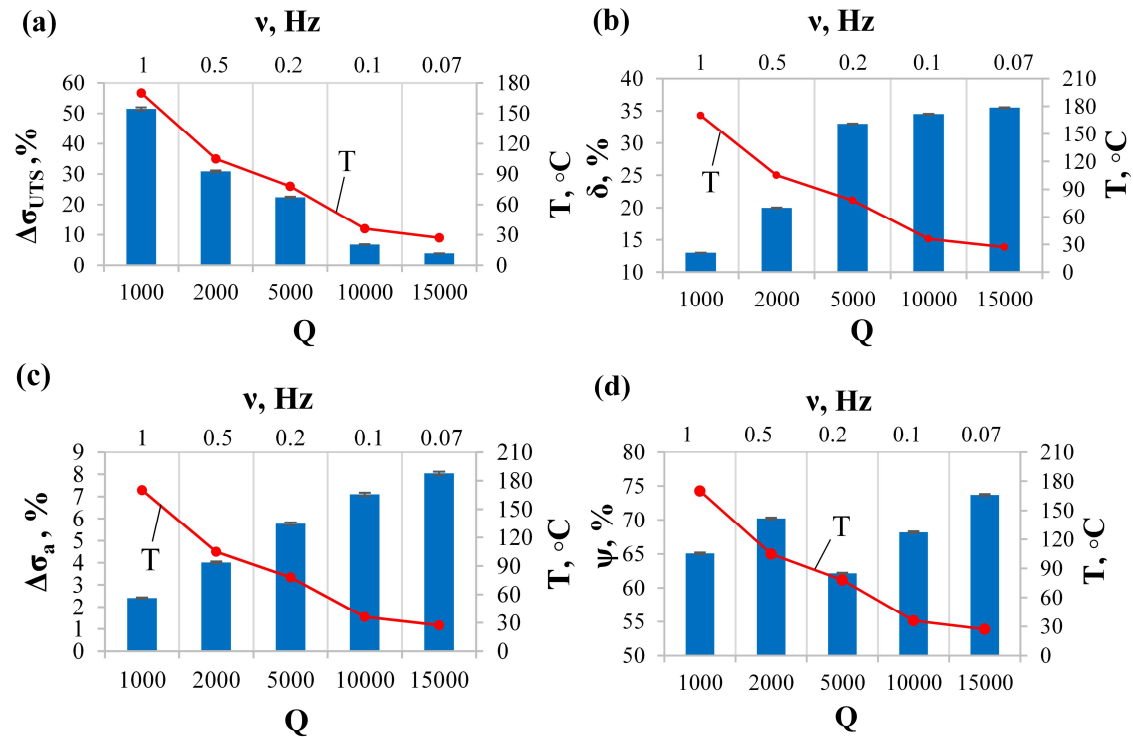
**Figure 3.** Stress–strain curves of titanium under tension without and with current ( $j = 1000$  A/mm<sup>2</sup>;  $\tau = 1000$   $\mu$ s) of different duty cycles: 1, no current; 2,  $Q = 15000$ ; 3,  $Q = 10000$ ; 4,  $Q = 5000$ ; 5,  $Q = 2000$ ; 6,  $Q = 1000$ .

Table 4 presents the mechanical properties and temperature of titanium under tension accompanied by a pulsed current for the modes in Table 2. A decrease in the duty cycle by an order of magnitude leads to an increase in the sample temperature from room temperature to 170 °C and a decrease in the ultimate strength and yield stress ( $\sigma_{0.2}$ ), elongation to failure ( $\delta$ ), reduction in area ( $\Psi$ ), and relative jump amplitude.

**Table 4.** Mechanical properties and test temperature of titanium.

No.	Condition	T (°C)	$\sigma_{0.2}$ (MPa)	$\sigma_{UTS}$ (MPa)	$\sigma_a$ (MPa)	$\Delta\sigma_a$ (%)	$\delta$ (%)	$\Psi$ (%)
1	No current	24 ± 2	203 ± 3	340 ± 3	-	-	35.5	81
2	Pulse current	27 ± 2	197 ± 3	327 ± 3	60 ± 3	8	35.5	73
3		36 ± 2	194 ± 3	317 ± 3	53 ± 3	7.1	34.5	68
4		78 ± 2	146 ± 3	264 ± 3	43 ± 3	5.8	33	62
5		105 ± 2	124 ± 3	235 ± 3	30 ± 3	4	20	70
6		170 ± 2	87 ± 3	165 ± 3	18 ± 3	2.4	13	65

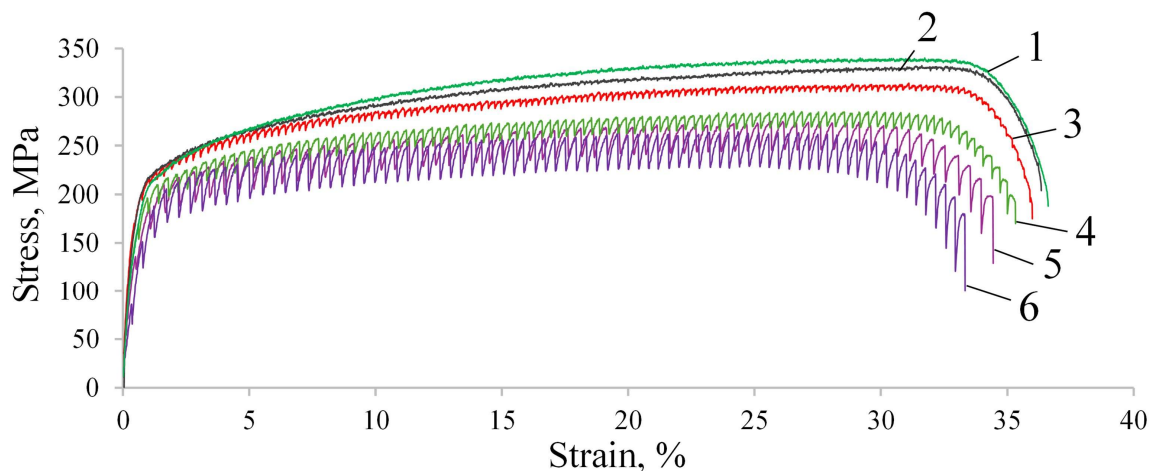
Figure 4 shows histograms of mechanical properties, relative jump amplitude, and temperature as functions of duty cycle at a constant pulse duration. It can be seen that as the duty cycle increases from 1000 to 15,000 (and the frequency decreases accordingly), the reduction in tensile strength decreases (Figure 4a), while the elongation to failure increases (Figure 4b), nearly reaching values corresponding to the no-current test. The relative jump amplitude (Figure 4c) reaches its maximum, and the temperature decreases to room temperature. A trend toward increasing reduction in area is also observed (Figure 4d).



**Figure 4.** Histograms of (a) ultimate strength change, (b) elongation to failure, (c) relative jump amplitude, (d) reduction in area, and (a–d) temperature from the duty cycle (at  $\tau = \text{Const}$ ) of the pulse current.

### 3.2. At a constant frequency

Figure 5 shows stress–strain curves without current and with currents of varying duty cycles (at the same frequency). As the duty cycle decreases by an order of magnitude (from 50000 to 5000), the yield stress and elongation to failure decrease, but the amplitude of the jumps increases (curves 2, 3, 4, 5, 6). The strain hardening coefficient, as in the previous case, decreases with decreasing duty cycle.



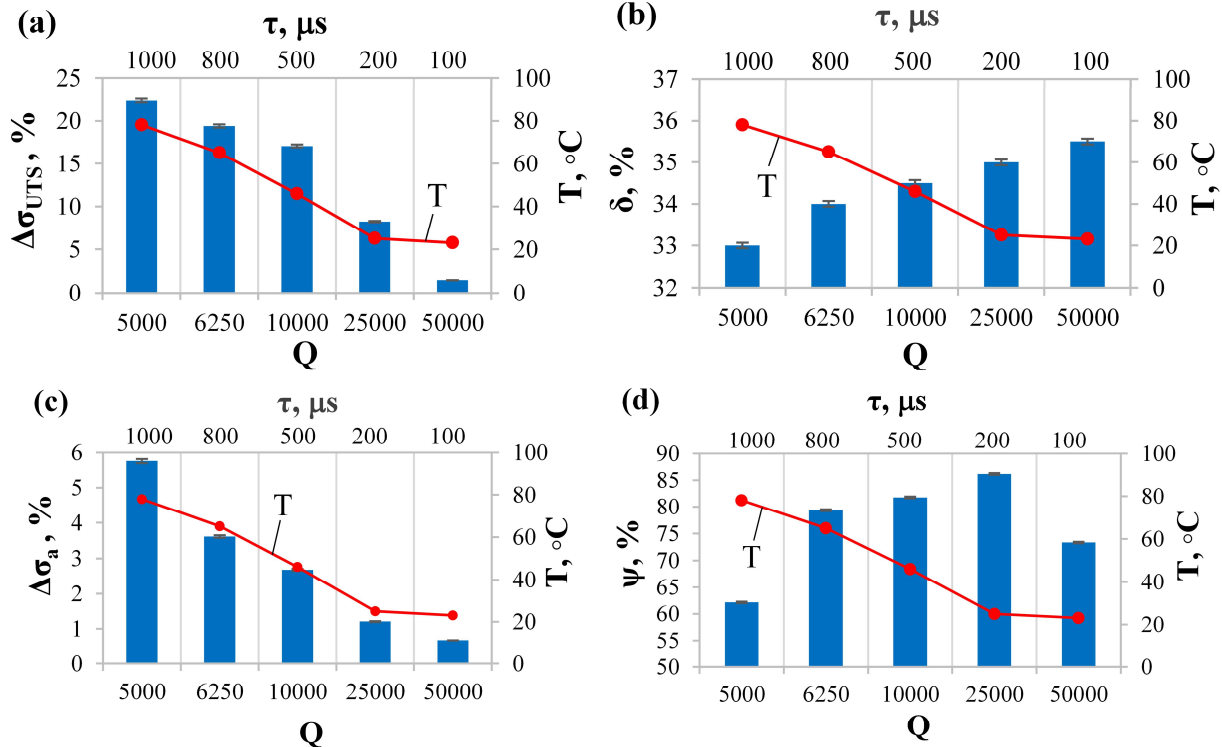
**Figure 5.** Stress–strain curves of titanium under tension without current and with current ( $j = 1000 \text{ A/mm}^2$ ;  $v = 0.2 \text{ Hz}$ ) of different duty cycles: 1, no current; 2,  $Q = 50000$ ; 3,  $Q = 25000$ ; 4,  $Q = 10000$ ; 5,  $Q = 6250$ ; 6,  $Q = 5000$ .

Table 5 presents the mechanical properties of titanium under tensile test with pulsed current for the conditions listed in Table 3. A decrease in the duty cycle is accompanied by an increase in the specimen temperature and a decrease in the ultimate tensile strength and yield stress. The relative jump amplitude ( $\Delta\sigma_a$ ) and elongation to failure ( $\delta$ ) change only slightly, unlike in previous tests. The reduction in area, however, decreases non-monotonically.

**Table 5.** Mechanical properties and test temperature for titanium.

No.	Condition	T (°C)	$\sigma_{0.2}$ (MPa)	$\sigma_{UTS}$ (MPa)	$\sigma_a$ (MPa)	$\Delta\sigma_a$ (%)	$\delta$ (%)	$\Psi$ (%)
1	No current	24 ± 2	203 ± 3	340 ± 3	-	-	35.5	81
2	Pulse current	24 ± 2	201 ± 3	335 ± 3	5 ± 3	0.7	35.5	73
3		25 ± 2	197 ± 3	312 ± 3	9 ± 3	1.2	35	86
4		46 ± 2	182 ± 3	282 ± 3	20 ± 3	2.7	34.5	65
5		65 ± 2	145 ± 3	274 ± 3	27 ± 3	3.6	34	79
6		78 ± 2	146 ± 3	264 ± 3	43 ± 3	5.8	33	62

Figure 6 shows histograms of mechanical properties, drop amplitude, and temperature as functions of duty cycle at a constant frequency. It can be seen that with increasing duty cycle (decreasing pulse duration), the reduction in tensile strength decreases, the elongation to failure and reduction in area reach values corresponding to a test without current, the stress drops amplitude decreases, and the temperature reaches room temperature.



**Figure 6.** Histograms of (a) ultimate strength, (b) elongation to failure, (c) relative jump amplitude, (d) reduction in area, and temperature (a, b, c, d) from the duty cycle (at  $v = \text{Const}$ ) of the pulse current.

### 3.3. Microhardness

Figure 7 shows histograms of microhardness measured for different current conditions in two zones: far from the fracture site (center) and near the fracture site (neck). Tension without current (sample 1) is characterized by an increase in microhardness in both zones compared to the initial undeformed state (see Materials and methods), with the increase being most pronounced in the neck. It is also evident that tension with current (samples 2 and 3 with high duty cycle) further increases microhardness in the neck. Reducing the duty cycle (samples 4, 5, and 6) leads to a decrease in microhardness in both zones to a level corresponding to sample 1 or even lower.

When comparing microhardness at the same duty cycle ( $Q = 10000$ ), obtained by different methods, one can note a stronger hardening in the neck, with a constant pulse duration.

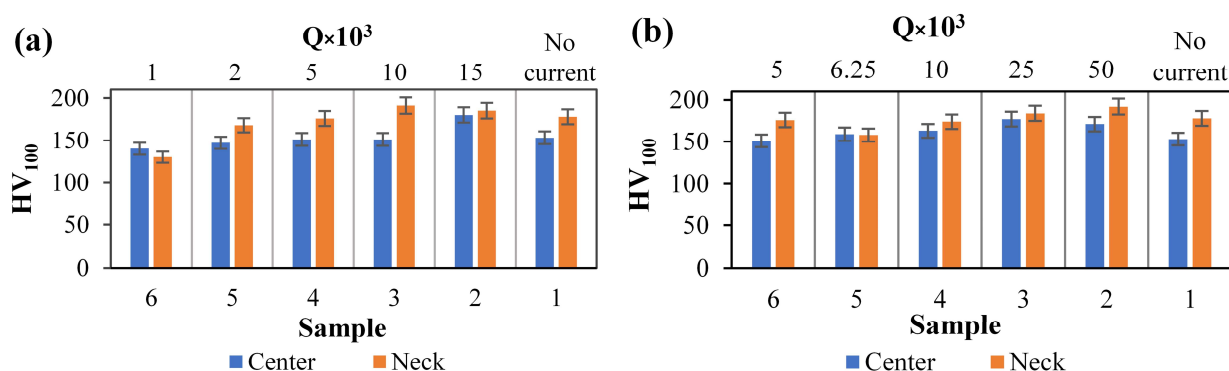


**Figure 7.** Histograms of microhardness with changing current duty cycle: (a) constant pulse duration; (b) constant frequency.

### 3.4. Microstructure

Figure 8 shows photographs of the microstructure for samples tested without current and with current at a reduced duty cycle. It is evident that tensile deformation without current is accompanied by intense twinning (95%), which is observed in virtually every grain (Figure 8a) and decreases (75%) upon introducing current at a duty cycle of  $Q = 10,000$  (Figure 8b). When the duty cycle is halved, the number of twins decreases sharply (10%), and twin-free grains appear (Figure 8c), while at the minimum duty cycle of  $Q = 1000$ , isolated twins (2%) are present only in individual grains (Figure 8d). The average grain size ( $200 \mu\text{m}$ ) remains virtually unchanged.

Thus, it is clear that the introduction of pulsed current helps to reduce the number of twinned grains and completely suppresses the twinning mechanism when the duty cycle is reduced from 10000 to 1000.

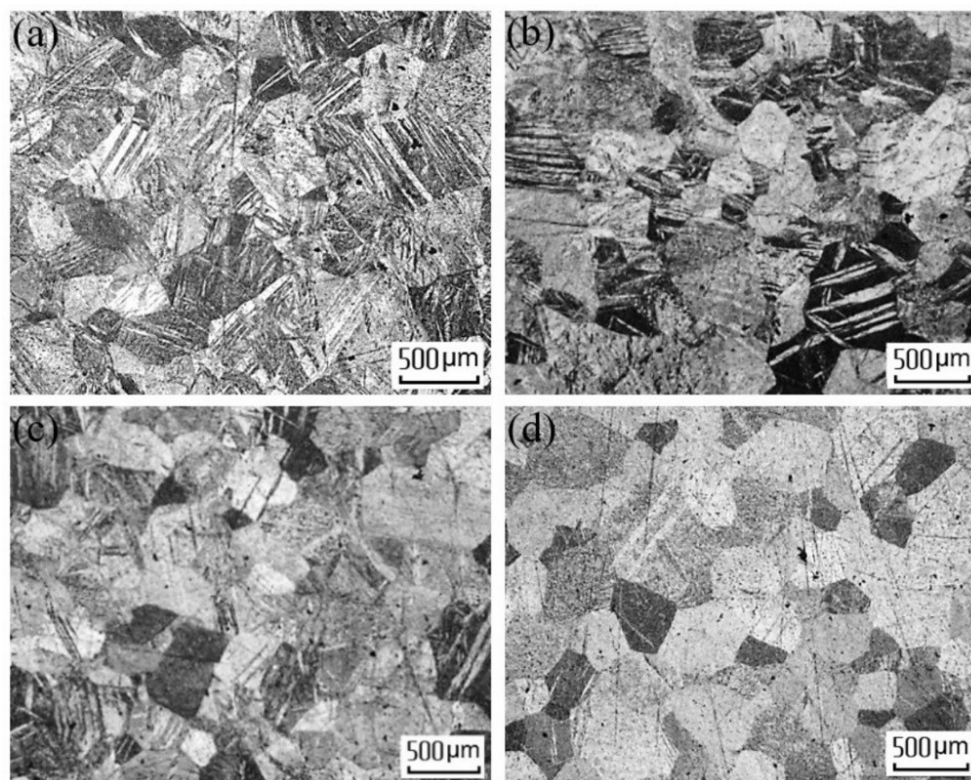


**Figure 8.** Microstructure of the working area of the samples: (a) number 1 (no current); (b) number 3,  $\tau = 1 \mu\text{s}$ ;  $Q = 10000$ ; (c) number 4,  $\tau = 1000 \mu\text{s}$ ,  $Q = 5000$ ; (d) number 6,  $\tau = 1000 \mu\text{s}$ ,  $Q = 1000$ .

### 3.5. Fractography

SEM images show that under tension without current, the fracture pattern is ductile, predominantly in the form of dimples approximately  $2 \mu\text{m}$  in size (Figure 9a). A current duty cycle of  $Q = 10000$  facilitates the disappearance of the dimples and the appearance of large cups bigger than  $20 \mu\text{m}$  in size (Figure 9b). Reducing the duty cycle leads to the appearance of isolated pores up to  $30 \mu\text{m}$  in size (Figure 9c). Further reductions in the duty cycle at the same pulse duration promote the formation of large pores up to  $100 \mu\text{m}$  in size and large cups (Figure 9d).

Thus, introducing a pulsed current during deformation affects the mechanism and nature of fracture. While ductile fracture persists, reducing the duty cycle from 10000 to 1000 promotes a change from a dimpled fracture to a cupped fracture, as well as the development of porosity.

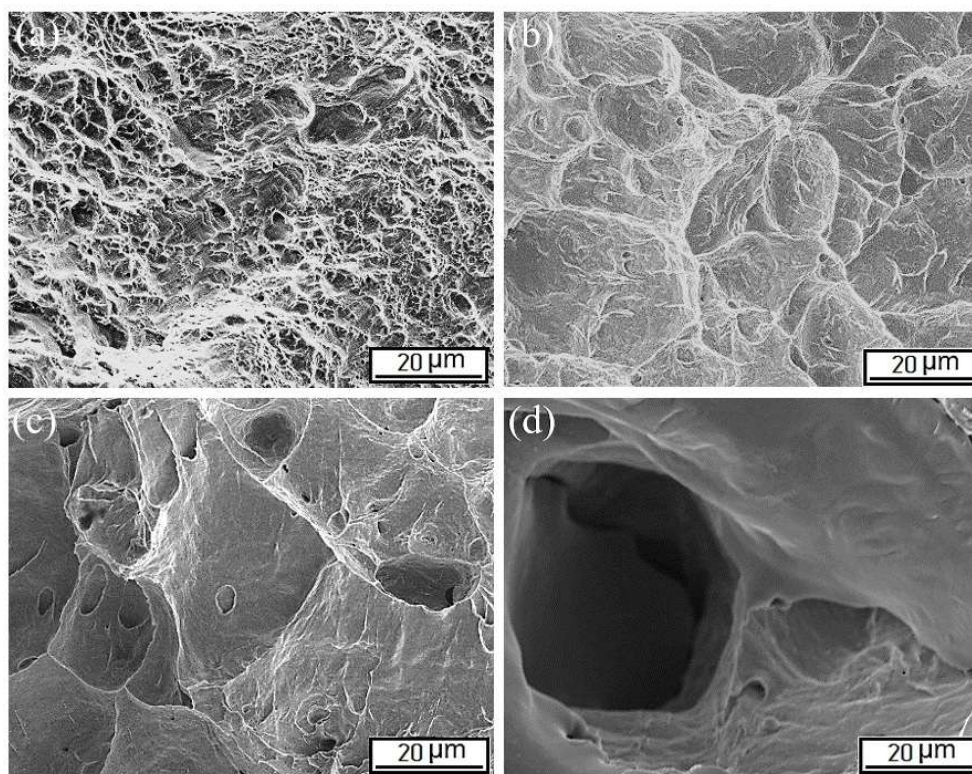


**Figure 9.** SEM images of the fracture zone: (a) number 1 (without current); (b) number 4,  $\tau = 500 \mu\text{s}$ ,  $Q = 10,000$ ; (c) number 4,  $\tau = 1000 \mu\text{s}$ ,  $Q = 5000$ ; (d) number 6,  $\tau = 1000 \mu\text{s}$ ,  $Q = 1000$ .

#### 4. Discussion

The results of this study, examining the influence of pulsed current on the deformation behavior, structure, and mechanical properties of coarse-grained titanium, indicate a strong influence of the duty cycle parameter over a wide range of values. One of the main reasons for this influence is related to the regulating function of the thermal contribution to the electroplastic effect. One may consider the specific influence of the pulsed current duty cycle.

The strain hardening coefficient  $\sigma_{0.2}/\sigma_{UTS}$  decreases from 0.6 to 0.5–0.55 with decreasing current duty cycle (see Tables 4 and 5), qualitatively demonstrating a decrease in the density of dislocations arising during deformation and an increase in the thermal contribution of the EPE. The shape of the stress–strain curves, accompanied by a low-duty-cycle pulsed current, confirms the achieved balance between hardening and softening processes in the horizontal area of the elastic-plastic zone.

The introduction of current pulses during tension is accompanied by downward stress drops, the amplitude of which depends on the duty cycle and can range from a few to tens of MPa at a constant current density. It was found that reducing the duty cycle at a constant pulse duration leads to a decrease in the drop amplitude, while at a constant frequency, it increases the drop amplitude. This opposing effect of the duty cycle is due to the different physical meanings of the kinetic parameters of pulse frequency and duration, which are included in the duty cycle formula.

The strength and ductility of titanium under a low-duty cycle pulsed current are reduced by more than half due to an increase in sample temperature and the accumulation of microdefects during low-cycle thermomechanical deformation.

Microhardness studies showed that its values are consistent with the behavior of strength characteristics. Due to the relief of internal stresses, microhardness decreases with decreasing duty cycle. Moreover, near the neck, it is always higher than farther from the fracture site due to localized deformation and microstructural refinement.

Microstructural changes during tension with and without current convincingly demonstrate that the mechanism of plastic deformation of titanium depends on the current and duty cycle. Deformation twins appear during tension without current and disappear when current is introduced, the more so the lower the duty cycle. This influence of current is associated with the competition between twinning and slip mechanisms with increasing temperature and was demonstrated in [11]. It should be noted that this fact is consistent with the strong negative temperature dependence of critical shear stresses (CRSS) for prismatic and pyramidal planes in alpha titanium known in the literature [12].

Fractographic studies showed that as the duty cycle decreases, the fracture morphology changes. The fracture type becomes predominantly cup-shaped, and pores form and grow within the cups. Thus, active pore formation may be one of the factors reducing elongation to failure.

Note that Figures 3 and 5 indicate an increase in temperature with a decrease in the duty cycle. However, the temperature increases faster with a change in pulse duration than with a change in frequency (for  $Q = 10000$ ). The mechanical properties depend on the method of changing the duty cycle in such a way that a change in frequency plays a more significant role. This is due to the amount of input energy, which decreases simultaneously with the pulse duration. For a more accurate calculation, method for determining the root means square (RMS) current density can be used, according to the formula from [13], which includes the exposure time (Eq 3):

$$j_{\text{rms}} = \frac{I \times \sqrt{\frac{\tau}{2t}}}{S} = j \times \sqrt{\frac{\tau}{2t}} \quad (3)$$

where  $S$  is the cross-sectional area of the sample,  $I$  is the amplitude current, and  $t$  is the period. The recalculated current parameters are given in Table 6.

**Table 6.** Root-mean-square current density.

$\nu$ (Hz)	$j$ (A/mm <sup>2</sup> )	$\tau$ (mks)	$Q$	$t$	$j_{\text{rms}}$ (A/mm <sup>2</sup> )	$T$ (°C)
0.07	1000	1	15,000	15	5.8	27
0.1			10,000	10	7.1	36
0.2			5000	5	10	78
0.5			2000	2	15.8	105
1			1000	1	22.4	170
0.2		100	50,000	5	3.2	24
		200	25,000		4.5	25
		500	10,000		7.1	46
		800	6250		8.9	65
		1000	5000		10	78

Based on the data shown in Table 6, it follows that reducing the duty cycle by changing the frequency contributes to a higher RMS current density. The difference in temperature with the same duty cycle and RMS current density is explained by the different current periods.

An increase/decrease in the duty cycle, regardless of its variation, is accompanied by an increase/decrease in the elongation to failure. This effect was also observed in previous studies on the tension of titanium alloys [10,14] at a duty cycle of 10, where the main explanation was active necking and the associated sharp increase in current density in the deformation zone. However, in the present study, the reduction in area decreases non-monotonically. At a duty cycle of 2000 and in the range of 6250–25,000, necking is less noticeable, which may be due to the suppression of prismatic and pyramidal slip. In addition, in [15], the influence of the current direction is considered so that when the current and deformation vectors coincide, the EPE is enhanced.

Experimental data showed that the effect of duty cycle on deformation behavior differs for changes in pulse duration or frequency. A characteristic of the effect of duty cycle due to frequency changes is a general decrease in flow stress, accompanied by a simultaneous reduction in the amplitude of the pulse surges. This can be interpreted as enough time to partially recover from flow stress at low frequencies (long periods), which is visible as high-amplitude drops on the stress–strain curve. As the frequency increases (the duty cycle decreases), more pulses are transmitted during the tension, which is accompanied by an increase in temperature. Moreover, the overall drop in flow stress under pulsed current is significantly greater than under thermal stress at the same temperatures, as confirmed by reference data for Grade 2 titanium [16].

The frequency of temperature sampling cannot guarantee an accurate temperature measurement at the moment of the pulse, so the measured temperature is somewhat lower than the actual temperature. To refine the obtained data, a high-speed infrared camera will be used in subsequent studies.

The effect of duty cycle due to changes in pulse duration is qualitatively similar to the previous case, but quantitatively differs in a less significant reduction in flow stress. This is apparently due to the fact that the thermal energy introduced into the samples in accordance with the Joule–Lenz law was lower than in the first case (with increasing frequency). This is confirmed by the difference in the thermal effect of the current (by temperature in Tables 3 and 5).

Thus, reducing the duty cycle leads to a significant reduction in strength and ductility properties, regardless of the method used to reduce the duty cycle. Reducing the duty cycle by increasing the frequency leads to a decrease in the amplitude of the downward stress drops. Conversely, reducing the duty cycle by increasing the pulse duration leads to an increase in the amplitude of the downward stress drops.

The histograms shown in Figures 3 and 5 suggest that varying the duty cycle is an effective way to control the thermal effect, with its increase reducing the thermal effect of the current and increasing the contribution of the EPE. Based on available literature data on thermal softening [16], the percentage softening was calculated for the temperatures obtained during the experiments. Subtracting this percentage from 100% yielded the nominal EPE effect. This calculation does not take into account other effects accompanying EPE (Figure 10).

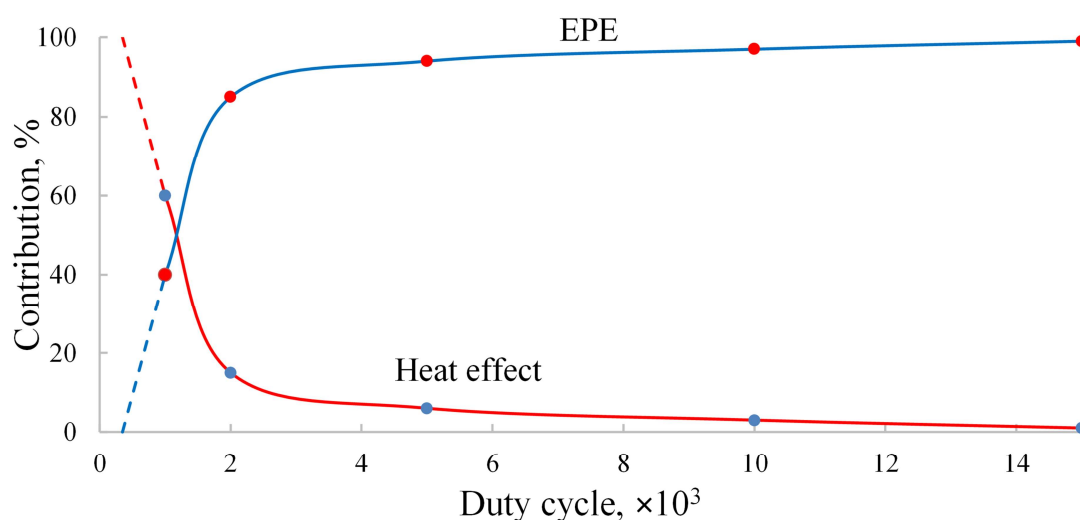


**Figure 10.** The influence of duty cycle on the ratio of EPE and thermal effect.

Interestingly, the dependences of the EPE contribution and the thermal effect change dramatically at  $Q = 2000$ . At  $10 < Q < 2000$ , a sharp decrease/increase in the thermal effect/EPE, respectively, occurs. At  $Q > 2000$ , both contributions change minimally.

## 5. Conclusions

1. Reducing the duty cycle increases temperature, reduces the stress drop amplitude, and reduces flow stress and elongation to failure. At the same time, area reduction tends toward a non-monotonous decrease.

2. For a given duty cycle, varying the frequency has a greater effect on mechanical properties and temperature than varying the pulse duration.

3. Using the duty cycle parameter allows one to control the contribution of thermal and true electroplastic effects, which can be useful both for modeling the EPE mechanism (at high  $Q$ ) and for practical use in current-assisted forming of titanium alloys (at low  $Q$ ).

4. Reducing the pulse current duty cycle in the range of  $Q = 10^3$ – $10^4$  in coarse-grained titanium during tension suppresses the primary deformation mechanism of twinning and activates predominantly sliding. The fracture mechanism remains ductile but shifts from dimple type to predominantly cup type, with a simultaneous increase in porosity.

## Use of AI tools declaration

The authors declare they have not used Artificial Intelligence (AI) tools in the creation of this article.

## Acknowledgments

This work was funded by a State Contract FFGU-2026-0003.

## Author contributions

Vladimir Stolyarov: supervision, revision, comments; Oleg Korolkov: experimental work, methodology, writing.

## Conflict of interest

The authors declare no conflict of interest.

## References

1. Kim MJ, Bui-Thi TA, Kang SG, et al. (2024) Electric current-induced phenomena in metallic materials. *Curr Opin Solid State Mater Sci* 32: 101190. <https://doi.org/10.1016/j.cossms.2024.101190>
2. Lv Y, Chen G, Zhang B, et al. (2024) Application of electroplastic effect in mechanical processing. *Int J Adv Manuf Technol* 135: 25–48. <https://doi.org/10.1007/s00170-024-14574-9>
3. Perkins TA, Kronenberger TJ, Roth JT (2006) Metallic forging using electrical flow as an alternative to warm/hot working. *J Manuf Sci Eng* 129: 84–94. <https://doi.org/10.1115/1.2386164>
4. Cao W, Sprecher AF, Conrad H (1989) Measurement of the electroplastic effect in Nb. *J Phys E Sci Instrum* 22: 1026. <https://doi.org/10.1088/0022-3735/22/12/015>
5. Pakhomov MA, Savenkov GG, Smakovsky MA, et al. (2023) Effect of pulsed current duty factor on deformation behavior of aluminum bronze. *Met Sci Heat Treat* 65: 292–297. <http://doi.org/10.1007/s11041-023-00928-9>
6. Stolyarov V (2026) Pulse current duty cycle and its role in the electroplastic effect of conductive materials. *J Mater Eng Perform*. <https://doi.org/10.1007/s11665-026-13355-7>
7. Kim MJ, Lee K, Oh KH, et al. (2014) Electric current-induced annealing during uniaxial tension of aluminum alloy. *Scr Mater* 75: 58–61. <https://doi.org/10.1016/j.scriptamat.2013.11.019>
8. Adabala S, Cherukupally S, Guha S, et al. (2022) Importance of machine compliance to quantify electro-plastic effect in electric pulse aided testing: An experimental and numerical study. *J Manuf Process* 75: 268–279. <https://doi.org/10.1016/j.jmapro.2021.12.027>
9. Gennari C, Calliari I, Stolyarov V (2020) Electroplastic effect in specimens of duplex stainless steel under tension. *Ind Lab Diagn Mater* 86: 41–45. <https://doi.org/10.26896/1028-6861-2020-86-10-41-45>
10. Li X, Xu Z, Guo P, et al. (2022) Electroplasticity mechanism study based on dislocation behavior of Al6061 in tensile process. *J Alloys Compd* 910: 164890. <https://doi.org/10.1016/j.jallcom.2022.164890>
11. Li H, Ding C, Xu Z. et al. (2025) Mechanical response and deformation mechanism of TA1 pure titanium during electrically assisted tension. *J Mater Res Technol* 39: 945–959. <https://doi.org/10.1016/j.jmrt.2025.09.077>
12. Khalikova GR, Korolkov OE, Stolyarov VV. et al. (2026) Competing deformation mechanisms of Grade 2 titanium under electrically assisted tension. *J Mater Res* 41: 494–507. <https://doi.org/10.1557/s43578-025-01768-4>

13. Tsukamoto G, Kunieda T, Yamasaki S, et al. (2021) Effects of temperature and grain size on active twinning systems in commercially pure titanium. *J Alloys Compd* 884: 161154. <https://doi.org/10.1016/j.jallcom.2021.161154>
14. Li X, Zhou Q, Zhao S, et al. (2014) Effect of pulse current on bending behavior of Ti6Al4V alloy. *Procedia Eng* 81: 1799–1804. <https://doi.org/10.1016/j.proeng.2014.10.235>
15. Stolyarov V, Korolkov O, Pesin A, et al. (2023) Deformation behavior under tension with pulse current of ultrafine-grain and coarse-grain CP titanium. *Materials* 16: 191. <https://doi.org/10.3390/ma16010191>
16. Chen C, Li C, Li C. et al. (2022) Effect of angle between pulse current and load direction on flow stress of Ti-6Al-4V alloy under uniaxial tension. *J Mater Eng Perform* 31: 9283–9293. <https://doi.org/10.1007/s11665-022-06921-2>
17. AZO Materials (2002) Titanium Alloys—Physical Properties. Available from: <https://www.azom.com/article.aspx?ArticleID=1341>.



AIMS Press

© 2026 the Author(s), licensee AIMS Press. This is an open access article distributed under the terms of the Creative Commons Attribution License (<https://creativecommons.org/licenses/by/4.0>)